Discussion of the Direct Detection Rx-power Distribution as derived from Intensity Statistics and Comparison with Measurements

N. Perlot, D.Giggenbach, H. Bischl, F. David

German Aerospace Center (DLR), D-82234 Wessling, Germany

ABSTRACT

The intensity of a laser beam after propagation through turbulent media such as the atmosphere may follow different probability density functions (PDFs) depending on the fluctuation regime. For non-coherent receivers the aperture averaging effect reduces the power scintillation leading to a different PDF. Since the analytical approach of deriving the received power PDF knowing the joint-PDF of the intensity at more than just a few points becomes rapidly complex, we review here a much more simplified approach as well as a simulative approach. Both approaches are based on the results of scintillation theory.

First, starting from the PDF of the intensity and its spatial correlation, aperture sub-areas can be defined over which the intensity is assumed equal and independent from other sub-areas' intensity. Under those conditions the power PDF is easily worked out. The validity of this method is evaluated according to the level of spatial correlation of the intensity. In a second method, intensity variables are sampled from the Rx-aperture and an approximation of the power PDF is obtained by generating multivariate correlated intensity values. Weak and strong fluctuation regimes are treated separately and the effects of different resolution of the input-intensity-field are discussed. In addition, this paper compares the predicted power characteristics to those deduced from experimental data where the intensity characteristics (PDF, spatial correlation) have been evaluated.

Keywords: aperture averaging, intensity distribution, optical scintillation, atmospheric turbulence, direct detection,

1. INTRODUCTION

After propagating through atmosphere the intensity of a laser beam is redistributed due to variations of the refractive index along the path. This phenomenon is called scintillation and the properties of the intensity fluctuations are described by scintillation theory. Scintillation is reduced at a direct detection receiver by increasing the collecting aperture over which the intensity is spatially averaged. The efficiency of aperture averaging depends on the spatial properties of the intensity in the receiver plane and the fluctuations of the received power have to be directly deduced from those of the intensity. Although there are other interesting aperture averaging effects such as the reduction of the fast fluctuations, we focus in this paper on deriving the power PDF from statistical properties of the intensity.

Considering a finite number of intensity variables disposed uniformly over the aperture, the statistically best way of relating the PDF of the intensity random variable and its spatial dependence would be to use the joint distribution of those variables. Although approximated expressions of the joint distribution may be found by means of the covariance matrix [1], the analytical way of finding the PDF of the sum of random variables (RVs) knowing their joint-PDF turns out to be greatly complex. In order to estimate the PDF of the spatial average intensity without going through too complex analytical expressions, two approaches were used. For both approaches comparisons are made with experimental data.

Author Contact: Nicolas.perlot@dlr.de
Nicolas Perlot, Institute of Communications and Navigation,
German Aerospace Center (DLR), Site Oberpfaffenhofen, D-82234 Wessling, Germany

2. INDEPENDENT SUB-APERTURE INTENSITIES

2.1 Convolution method

By dividing the Rx-aperture into sub-apertures over which the intensity is assumed fully correlated, the power contained in each sub-aperture can be directly described by the intensity (Fig.1). We then assume these sub-aperture powers to be independent of each other. If the sub-apertures have equal areas, the PDF of the total collected power is deduced from the convolution of every intensity PDF. Considering the n independent intensity variables I_1, I_2 … I_n, the PDF of their sum is given by

$$P_{I_1+I_2+\ldots+I_n}(I) = P_{I_1}(I) * P_{I_2}(I) * \ldots * P_{I_n}(I) \tag{1}$$

where $P_{I_i}(I)$ is the PDF of the intensity variable I_i.

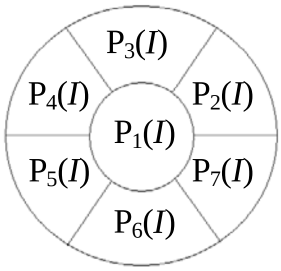

Fig. 1: Division of the receiver aperture into 7 sub-apertures.

Letting I_1, I_2 … I_n represent the intensity of the n sub-apertures, the received power Pow is

$$Pow = \frac{(I_1 + I_2 + \ldots + I_n)}{n} S \tag{2}$$

where S is the area of the complete receiving aperture. The power PDF follows as

$$P_{pow}(Pow) = P_{I_1+I_2+\ldots+I_n}\left(\frac{n}{S} Pow\right)\frac{n}{S} \tag{3}$$

Assuming furthermore that the intensity variables I_1, I_2 … I_n are identically distributed, the power variance is directly deduced from the intensity variance:

$$\mathrm{var}(Pow) = \left(\frac{S}{n}\right)^2 \mathrm{var}(I_1 + I_2 + \ldots + I_n) = \frac{S^2}{n}\mathrm{var}(I) = \frac{\mathrm{var}(S \cdot I)}{n} \tag{4}$$

with $I = I_i, \quad i \in \{1, 2, \ldots, n\}$

The aperture averaging factor A defined by the ratio of the irradiance flux variance obtained by a finite-size collecting lens to that obtained by a 'point aperture' is thus $A = 1/n$. This simple approach has been used for approximating power statistics of laser speckles [2] and is similar to the prediction of the power PDF when multiple beams propagating independently through the atmosphere overlap at the receiver [3].

The appropriate size of the sub-apertures (and thus, also the appropriate number of convolutions) can be roughly estimated by equating the effective sub-area radius r_{eff} to the intensity correlation radius ρ_c. The correlation radius is a measure of the spatial distance from a point in the wavefront plane to which surrounding points are spatially correlated. ρ_c can be estimated from scintillation theory: it is known that under weak fluctuations the correlation radius is on the order of the first Fresnel zone, while for an optical wave experiencing stronger turbulence conditions and multiple scattering, the correlation radius follows the behavior of the spatial coherence radius [4]. However, defining the correlation radius as the $1/e^2$ crossing point of the normalized spatial covariance function of the intensity, the determination of the number of sub-areas from only the correlation radius may not lead to the best results. Indeed, the optimal number of sub-areas is given by the optimal aperture averaging factor *A*, which depends on the shape of the normalized covariance function. Assuming a statistically homogeneous and isotropic optical field, *A* is given by [5]:

$$A = \frac{16}{\pi D^2} \int_0^D b(\rho) \left[\cos^{-1}\left(\frac{\rho}{D}\right) - \left(\frac{\rho}{D}\right) \sqrt{1 - \left(\frac{\rho}{D}\right)^2} \right] \rho d\rho \tag{5}$$

where $b(\rho)$ is the normalized covariance function and *D* the diameter of the circular aperture. Thus, if *A* is available the optimal number of sub-areas is found by rounding $1/A$.

2.2 Comparison with experimental data

We compare here the results given by this method with experimental data from a 1.3 km horizontal ground-to-ground link. The experiment features an average height above ground of 12 meters and high temperatures leading to strong turbulence conditions with a C_n^2 evaluated to 1.2×10^{-13} $m^{-2/3}$ and an inner and outer scale evaluated respectively to l_0 = 5 mm and L_0 = 2.5 m [6]. The wavelength of the laser beam was 980 nm and a spherical wave model could be assumed. The field was collected by a circular aperture with diameter *D* = 75 mm. The spherical wave Rytov variance defined by [5]

$$\beta_0^2 = 0.5 C_n^2 k^{7/6} L^{11/6} \tag{6}$$

is in this case $\beta_0^2 = 2.7$, testifying to strong fluctuation regime.

Several intensity PDF models have been developed for the strong-fluctuation regime. For this scenario we used the gamma-gamma PDF model whose parameters can be directly related to the atmospheric conditions. The gamma-gamma distribution is derived from a modified Rytov theory and its expression is [4]:

$$P(I) = \frac{2(\alpha\beta)^{(\alpha+\beta)/2}}{\Gamma(\alpha)\Gamma(\beta) I} \left(\frac{I}{< I >}\right)^{(\alpha+\beta)/2} K_{\alpha-\beta}\left(2\sqrt{\frac{\alpha\beta I}{< I >}}\right), \qquad I > 0, \tag{7}$$

where $\langle I \rangle$ is the mean intensity and the two parameters α and β are related to large-scale scintillation and small-scale scintillation respectively.

The parameters corresponding to the experimental scenario are $\alpha = 1.055$, $\beta = 1.390$. To avoid error introduced by the estimation of a parameter that is irrelevant to the assessment of this method, $\langle I \rangle$ was set to the experimental mean intensity ($\langle I \rangle = 4.22\times10^{-4}$ W/m^2). The normalized intensity variance, or scintillation index, predicted by the modified Rytov theory is $\sigma_I^2 = (\alpha+\beta+1)/\alpha\beta = 2.350$.

The power PDFs resulting from different numbers of convolutions are plotted along with the distribution of the experimental data in Fig. 2. The spatial normalized covariance functions that this method supposes, are shown in Fig. 3 as well as the zero-inner-scale covariance model for a spherical wave [4]. From Fig.3, the best approximation of the experimental distribution is the one resulting from 5 independent sub-apertures and supposing an aperture averaging factor of *A* = 1/5 = 0.2. Based on an ABCD matrix formulation of an optical system with one lens the method developed by Andrews et al. [7] predicts an aperture averaging factor of *A* = 0.223 for this scenario. Eventually the value of *A* calculated from (5) with $b(\rho)$ taken as the covariance function model plotted in Fig. 3, is *A* = 0.164. The underestimation of the aperture averaging factor by formula (5) can be assigned to the absence of inner scale in the covariance function model. As for the effective radius of a sub-aperture, we get r_{eff} = 16.8 mm, which is 56% of the correlation radius (derived as the $1/e^2$ crossing point of the covariance function model). This percentage would certainly be lower for a nonzero inner scale model.

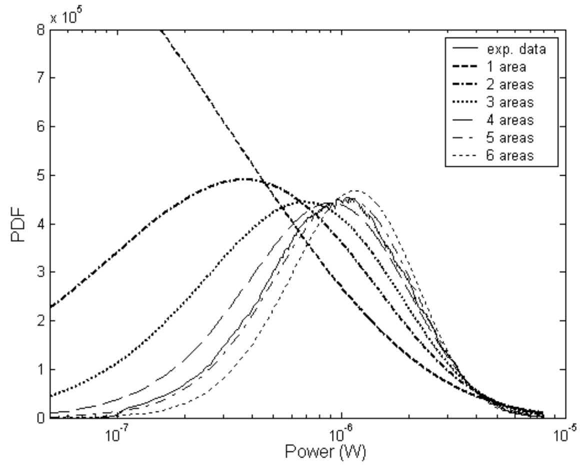

Fig. 2: Distribution of experimental power and power PDFs resulting from convolutions of intensity PDFs

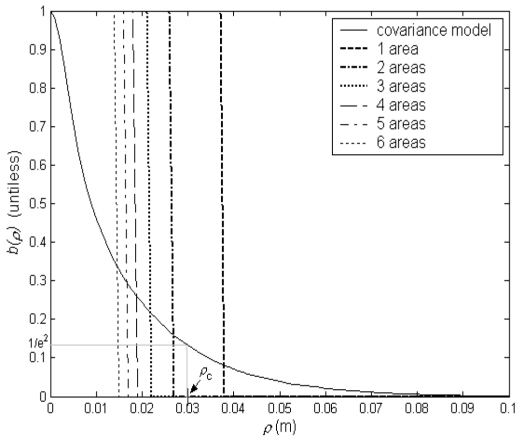

Fig. 3: Normalized spatial covariance functions of irradiance. The zero-inner scale covariance function model from [4] is plotted along with those induced by different numbers of independent sub-apertures

2.3 Critics and limitations

Provided that the intensity PDF for various propagation conditions and the aperture averaging factor are known, the convolution method can be easily applied for any scenario. The actual shape of the PDF is reached only in limiting cases: if there is no aperture averaging, intensity PDF is equivalent to power PDF and if the correlation radius becomes very small compared to the aperture size, the power PDF resulting from convolutions approaches the actual power PDF by virtue of the central limit theorem. However, because this method binarizes the intensity spatial correlation, it is little respectful of the pattern spatial properties and provides generally a bad fit of the low power values.

3. CORRELATED SUBAPERTURE INTENSITIES

3.1 Overview of simulation approach

By generating stochastic processes featuring the statistical spatial and temporal properties of the intensity, we can simulate the behavior of the intensity at points distributed all over the aperture. The aperture averaging process then simply results in adding the values of the stochastic processes for each point. The PDF and the temporal spectrum of the received power would be found simply by analyzing the resulting stochastic vector. However the difficulty resides here in generating different stochastic processes with the correct spatial and temporal correlation.

Taking interest only in the PDF, we want to do the averaging over the intensity variables by generating intensity values for different points of the aperture. The uniform spatial sampling of the aperture enables to give the same weight to each intensity variable. To introduce spatial correlation between those intensity values, we use the covariance matrix of the considered variables (Fig. 4). The covariance matrix depicts only the second central moments, but for simplicity reasons and, above all, lacking further information on spatial dependency, we will ignore the higher moment orders. The particular case of the lognormal PDF is considered as well as a more general approach, in which the gamma-gamma PDF is put forth. In both approaches we first generate correlated normal variables. Those normal variables are then converted into variables with the desired distribution. The properly correlated intensity values of each aperture realization are then summed.

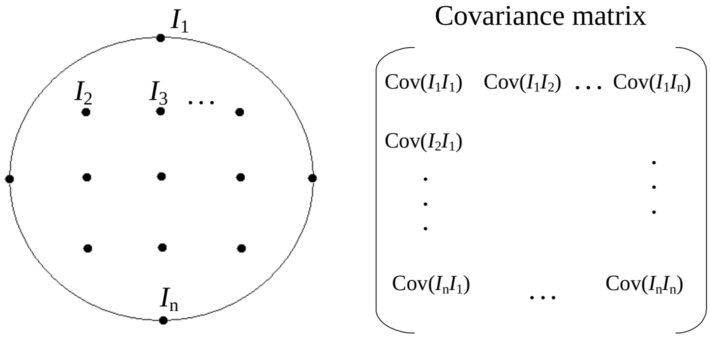

Fig. 4: Averaging of correlated intensities defined at points distributed all over the aperture

3.3 Generation of correlated normal random variables

To generate the normal RVs featuring a zero mean and a covariance matrix $\mathbf{C}_Y$ we use the Cholesky factorization of $\mathbf{C}_Y$ [8]. So we obtain correlated normal variables Y_1, Y_2 ,… Y_n by means of the operation $\mathbf{Y} = \mathbf{XT}$, where $\mathbf{Y}$ is the vector (Y_1 Y_2 … Y_n), $\mathbf{X}$ is a vector of independent standard normal variables and $\mathbf{T}$ is the triangle matrix given by $\mathbf{C}_Y = \mathbf{T'T}$.

3.4 Generation of correlated lognormal random variables

We know that for weak scintillation (scintillation index small compared to unity) the intensity PDF is lognormal [5]:

$$P(I) = \frac{1}{I\sqrt{2\pi\sigma_I^2}} \exp\left\{ -\frac{\left[\ln\left(\frac{I}{<I>} \right) + \frac{1}{2}\sigma_I^2 \right]^2}{2\sigma_I^2} \right\}, \qquad I > 0, \tag{8}$$

where $<I>$ is the mean intensity and σ_I^2 the scintillation index

To obtain lognormal RVs from normal RVs we use the simple transformation $I = \exp(Y)$. Through this transformation the covariance matrix of the RVs is not preserved. Under the assumption that every RV has the same PDF (same mean and variance) a correspondence between the covariance matrices of $\mathbf{I}$ and $\mathbf{Y}$ is easily found:

$$C_Y(i,j) = \ln\left(\frac{C_I(i,j)}{<I>^2} + 1 \right), \qquad (i,j) \in \{1,2,\ldots,n\}^2 \tag{9}$$

The corresponding mean value of the normal variables Y_i, that must be used for their generation is

$$<Y_i> \; = \ln(<I>) - \frac{1}{2}\sigma_I^2 \tag{10}$$

3.5 Generation of correlated gamma-gamma random variables

The method used here can actually be applied to RVs having arbitrary marginals. Because of its attractiveness the gamma-gamma marginal is nonetheless hypothesized in this section. Should the marginal of the intensity variable be modeled by a K distribution, as it has been proposed in [5], there exist certain procedures to generate such correlated RVs [9][10].

To find the required covariance coefficients of the normal variables before the transformation, like in the section 3.4, we use a search algorithm. For the sake of simplicity we consider normalized variables Y_i here, so that they become standard normal variables with $C_Y(i,i) = 1$. The correlated standard normal RVs Y_i are converted to intensity variables I_i with gamma-gamma marginal distribution through the following transformation [8]:

$$I_i = F_{gg}^{-1}\cdot\left[\frac{1}{2}\operatorname{erf}\left(\frac{Y_i}{\sqrt{2}}\right)+\frac{1}{2}\right] \tag{11}$$

where F_{gg}^{-1} is the inverse gamma-gamma cumulative distribution function.

Given the covariance matrix $\mathbf{C}_Y$, the joint distribution of $\mathbf{Y}$, defined in the sense of entropy maximization, is the multivariate Gaussian [8]

$$P(\mathbf{Y}) = \frac{1}{(2\pi)^{n/2}\sqrt{\det(\mathbf{C}_Y)}}\cdot\exp\left(-\frac{1}{2}\mathbf{Y}^t\mathbf{C}_Y^{-1}\mathbf{Y}\right) \tag{12}$$

From the joint distribution of the variables Y_i, we derive the joint distribution of the variables I_i:

$$P(\mathbf{I}) = P(\mathbf{Y})\cdot\left|\frac{\partial\mathbf{Y}}{\partial\mathbf{I}}\right| \tag{13}$$

where $\left|\frac{\partial\mathbf{Y}}{\partial\mathbf{I}}\right|$ is the Jacobian of the **Y** to **I** transformation.

From (11) we can write

$$\frac{\partial Y_i}{\partial I_j} = \sqrt{2\pi}P_j(I_j)e^{\frac{1}{2}Y_i^2}\delta_{ij} \tag{14}$$

and thus

$$\left|\frac{\partial\mathbf{Y}}{\partial\mathbf{I}}\right| = (2\pi)^{n/2}\prod_{i=1}^{n}P(I_i)e^{\frac{1}{2}Y_i^2} \tag{15}$$

leading to

$$P(\mathbf{I}) = \frac{1}{\sqrt{\det(\mathbf{C}_Y)}}\exp\left(-\frac{1}{2}\mathbf{Y}^t\left(\mathbf{C}_Y^{-1}-\mathbf{Id}\right)\mathbf{Y}\right)\prod_{i=1}^{n}P(I_i) \tag{16}$$

where **Id** is the $n\times n$ identity matrix. We therefore have related the covariance matrix $\mathbf{C}_Y$ to the intensity joint distribution $P(\mathbf{I})$. Restricting our number of variables to two and considering one covariance coefficient at a time, we then search for the value of $\mathrm{cov}(Y_1,Y_2)$ that will give us the desired intensity covariance coefficient $\mathrm{cov}(I_1,I_2)$. It should be mentioned that this correspondence is not valid for every marginal distribution. Assuming the correspondence exists, the intensity covariance coefficients related to the $\mathrm{cov}(Y_1,Y_2)$ candidate values are calculated numerically from their definitions

$$\mathrm{Cov}\left(I_i,I_j\right) = \int_0^{+\infty}\int_0^{+\infty} I_i I_j P_{I_iI_j}(I_i,I_j)\,dI_i\,dI_j - \langle I_i\rangle\langle I_j\rangle \tag{17}$$

The required covariance of (Y_i, Y_j) is then reached by simple dichotomy. Because the gamma-gamma cumulative distribution function has no tractable expression, tabulated values along with interpolations may be used for this transformation [11].

3.4 Comparison with experimental data

Applying this approach to the scenario mentioned in 2.2, different grid resolutions have been assessed. These are shown in Table 1 and are characterized by the minimum distance $\rho_{\min}$ between two intensity variables. The random intensity values were generated in a way that their covariance matrix fits the zero-inner-scale covariance model for a spherical wave. For each resolution, Table 1 shows the normalized covariance coefficients of the generated variables along with the normalized covariance model $b(\rho)$ and displays the corresponding aperture averaging factor.

$\rho_{\min} = D/2$, 5 points	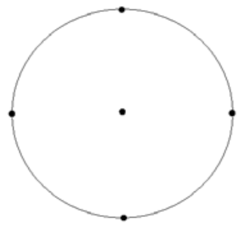	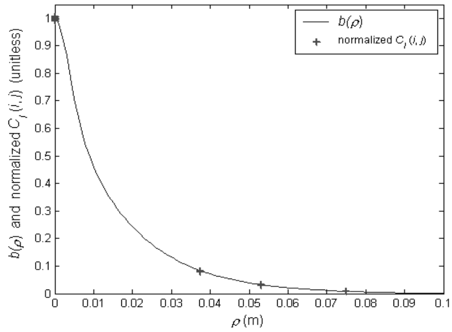	$A = 0.236$
$\rho_{\min} = D/4$, 13 points	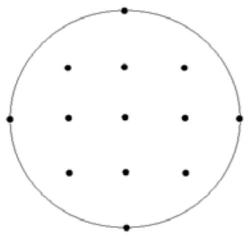	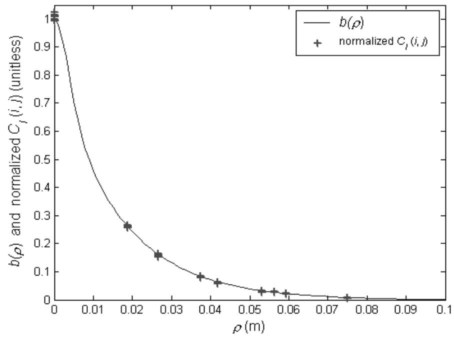	$A = 0.181$
$\rho_{\min} = D/6$, 29 points	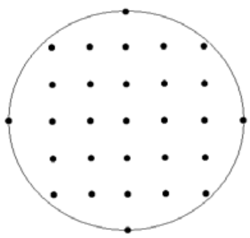	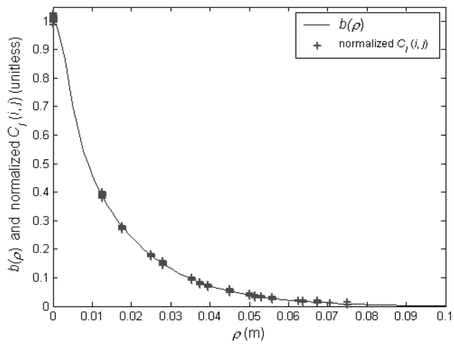	$A = 0.163$
$\rho_{\min} = D/8$, 49 points	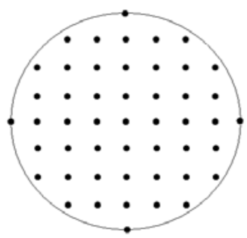	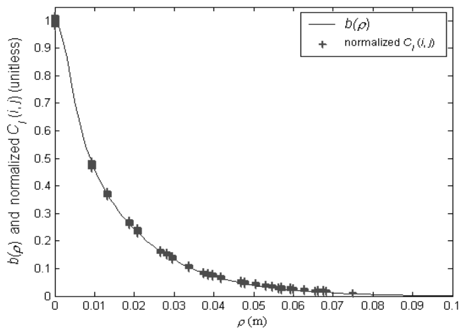	$A = 0.168$

Table 1: For each considered resolution of aperture sampling, normalized covariance coefficients of the generated data are plotted along with the exploited normalized covariance model and calculated aperture averaging factor

Ideally the aperture averaging factor should reach the previously computed value $A = 0.164$. Having a correlation radius about $\rho_c \approx D/3$ for this scenario, we see that, as long as $\rho_{\min}$ is bigger than the correlation radius, the resolution is insufficient to correctly approximate the aperture averaging. On the contrary, choosing a small $\rho_{\min}$ will fit $b(\rho)$ for low values of ρ but may lead to a consequential number of variables.

The power PDFs calculated from the summation of the generated intensities are shown in Fig. 5. In Fig. 6, the power distribution of the measured data is compared to the power distribution from simulated data with the best considered resolution. Again a primary reason for the observed discordance between measured and predicted PDF is likely to be the absence of inner scale (and, in a less extent, of outer scale) in the exploited covariance model.

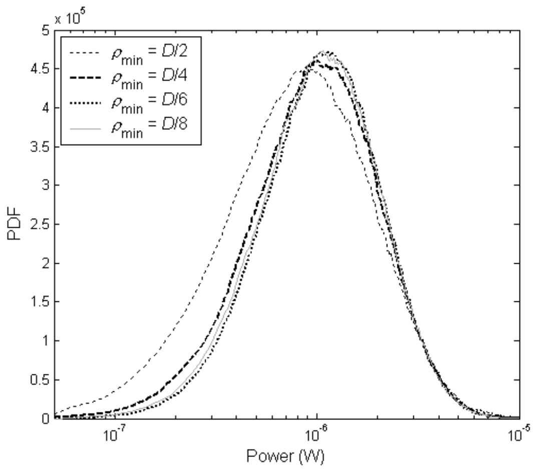

Fig. 5: Power PDFs from the generation of correlated data

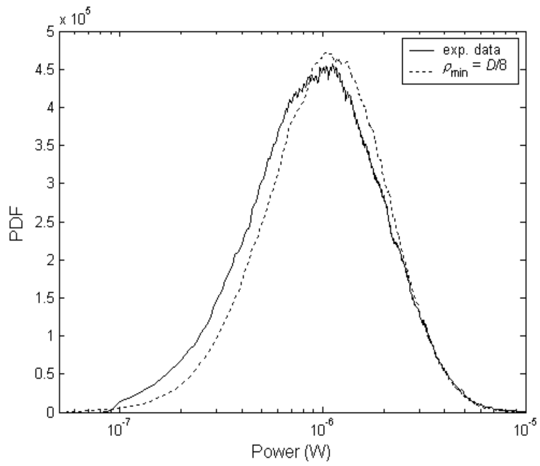

Fig. 6: Power distribution from measurements and power distribution from the generation of correlated data with $\rho_{\min} = D/8$

3.5 Critics and limitations

Whatever the fluctuation regime or the size of the aperture with respect to the correlation radius may be, the PDF approximation gets clearly better as the resolution distance $\rho_{\min}$ reaches the correlation radius.

Although several coefficients within the covariance matrix have the same value and thus the search algorithm does not need to be repeated for each coefficient, an accurate computation of the C_y coefficients may require time. Moreover as the size of the covariance matrix increases the number of generated samples required to obtain correctly correlated data also increases. Hence, the available memory may be a restriction to the achievement of accurate data.

4. CONCLUSIONS

We reviewed two approaches to derive the PDF of the power collected by a direct-detection receiver. Because of the analytical complexity of the problem, only numerical and approximated predictions of the power PDF were carried out. The results, which rely strongly on the models developed by the scintillation theory, are apparently well supported by experimental data.

REFERENCES

[1] X. Zhu and J. M. Kahn, “Free-Space Optical Communication through Atmospheric Turbulence Channels”, *IEEE Transactions on Communications*, 2002.

[2] J.W. Goodman, “Statistical properties of laser speckle patterns”, in Topics in Applied Physics, vol. 9, *Laser Speckle and related Phenomena*, editor: J.C. Dainty, N-Y, 1975.

[3] M. Jeganathan, M. Toyoshima, K. Wilson, J. James, G. Xu and J. Lesh "Data analysis results from the GOLD laser communications demonstration", Proc. SPIE, **2990**, *Free-Space Laser Communication Technologies*, 70-81, 1997.

[4] L.C. Andrews, R.L.Phillips, C. Y. Hopen, *Laser Beam Scintillation with application*, SPIE Press, Bellingham (WA), USA, 2001.

[5] L.C. Andrews, R.L.Phillips, *Laser Beam Propagation through Random Media*, SPIE Press, Bellingham (WA), USA, 1998.

[6] R.R. Beland, "Propagation through atmospheric optical turbulence," in The Infrared and Electro-Optical Systems Handbook, SPIE Press, 1993.

[7] L. C. Andrews, R. L. Phillips, C. Y. Hopen, "Aperture averaging of optical scintillations: power fluctuations and the temporal spectrum", *Waves Random Media* **10**, pp. 53-70, 2000.

[8] A. Papoulis, *Probability, Random Variables, and Stochastic Processes*, 3rd ed. (McGraw-Hill, Inc) , 1991.

[9] D. Blacknell, "New method for the simulation of correlated K-distributed clutter", *IEEE Proc.-Radar, Sonar Navig.*, Vol.141, No.1, pp. 53-58, 1994.

[10] O. H. Bustos, A. G. Flesia, A. C. Frery, "Generalized Method for Sampling Spatially Correlated Heterogeneous Speckled Imagery", *EURASIP Journal on Applied Signal Processing*, pp. 89-99, 2001.

[11] M. C. Jeruchim, P. Balaban, K. S. Shanmugan, *Simulation of communication systems*, Plenum Press, New York, 1992.